pH-Dependent Transfer Hydrogenation of Ketones with HCOONa as a Hydrogen Donor Promoted by (η^6-C_6Me_6)Ru Complexes

Seiji Ogo,*,† Tsutomu Abura,†,‡ and Yoshihito Watanabe*,§

Department of Material and Life Science, Graduate School of Engineering, Osaka University, Suita, Osaka 565-0871, Japan, Department of Structural Molecular Science, The Graduate University for Advanced Studies, Myodaiji, Okazaki 444-8585, Japan, and Department of Chemistry, Graduate School of Science, Nagoya University, Chikusa-ku, Nagoya 464-8602, Japan

Received December 14, 2001

The paper reports on the development of a new class of water-soluble organometallic catalysts for pH-dependent transfer hydrogenation. An organometallic aqua complex [(η^6-C_6Me_6)Ru^{II}(bpy)(H_2O)]$^{2+}$ (**1**, bpy = 2,2′-bipyridine) acts as a catalyst precursor for pH-dependent transfer hydrogenation of water-soluble and -insoluble ketones with HCOONa as a hydrogen donor in water and in biphasic media. Irrespective of the solubility of the ketones toward water, the rate of the transfer hydrogenation shows a sharp maximum around pH 4.0 (in the case of biphasic media, the pH value of the aqueous phase is adopted). In the absence of the reducible ketones, as a function of pH, complex **1** reacts with HCOONa to provide a formato complex [(η^6-C_6Me_6)Ru^{II}(bpy)(HCOO)]$^+$ (**2**) as an intermediate of β-hydrogen elimination and a hydrido complex [(η^6-C_6Me_6)Ru^{II}(bpy)H]$^+$ (**3**) as the catalyst for the transfer hydrogenation. The structures of **1**(PF_6)$_2$, **2**(HCOO)·HCOOH, and [(η^6-C_6Me_6)Ru^{II}(H_2O)$_3$]SO_4·3H_2O {**4**(SO_4)·3H_2O}, the starting material for the synthesis of **1**, were unequivocally determined by X-ray analysis.

Introduction

The interest in water-soluble organometallic complexes is becoming significant because of many potential advantages such as alleviation of environmental problems associated with the use of organic solvents, industrial applications (e.g., introduction of new biphasic processes), and reaction-specific pH selectivity.[1] Recently, we have reported pH-dependent reductions of water-soluble compounds promoted by water-soluble Cp*Ir (Cp* = η^5-C_5Me_5) complexes.[2] Herein, we report development of a new class of water-soluble organometallic catalysts for the pH-dependent transfer hydrogenation.[3] An organometallic aqua complex [(η^6-C_6Me_6)-Ru^{II}(bpy)(H_2O)]$^{2+}$ (**1**, bpy = 2,2′-bipyridine)[4] acts as a catalyst precursor for the pH-dependent transfer hydrogenation of water-soluble and -insoluble ketones with HCOONa as a hydrogen donor in water and in biphasic media, respectively. A conceivable mechanism for the pH-dependent transfer hydrogenation promoted by **1** as the catalyst precursor, a formato complex [(η^6-C_6Me_6)-Ru^{II}(bpy)(HCOO)]$^+$ (**2**) as an intermediate of β-hydrogen elimination,[5] and a hydrido complex [(η^6-C_6Me_6)Ru^{II}-(bpy)H]$^+$ (**3**) as the catalyst is proposed (Scheme 1).

Results and Discussion

Starting Material [(η^6-C_6Me_6)Ru^{II}(H_2O)$_3$]$^{2+}$ (4). A triaqua complex [(η^6-C_6Me_6)Ru^{II}(H_2O)$_3$]SO_4 {**4**(SO_4)}[6] appears to be a potential synthon for the preparation of many types of (η^6-C_6Me_6)Ru complexes in water. We here disclose the crystal structure of **4**(SO_4)·3H_2O by X-ray analysis (Figure 1).[7] Complex **4** has a distorted-octahedral structure with a piano stool geometry formed

* To whom all correspondence should be addressed.
† Osaka University. E-mail: ogo@ap.chem.eng.osaka-u.ac.jp.
‡ The Graduate University for Advanced Studies.
§ Nagoya University.

(1) (a) Cornils, B.; Herrmann, W. A. In *Aqueous-Phase Organometallic Catalysis*; Wiley-VCH: Weinheim, 1998; p 615. (b) Li, C.-J.; Chan, T.-H. In *Organic Reactions in Aqueous Media*; John Wiley & Sons: New York, 1997; p 199. (c) Horváth, I. T.; Joó, F. In *Aqueous Organometallic Chemistry and Catalysis*; Kluwer Academic Publishers: Dordrecht, 1995; p 317. (d) Joó, F.; Kathó, Á. *J. Mol. Catal. A* **1997**, *116*, 3−26. (e) Koelle, U. *Coord. Chem. Rev.* **1994**, *135/136*, 623−650. (f) Herrmann, W. A.; Kohlpaintner, C. W. *Angew. Chem., Int. Ed. Engl.* **1993**, *32*, 1524−1544.

(2) (a) Ogo, S.; Makihara, N.; Watanabe, Y. *Organometallics* **2001**, *20*, 4903−4910. (b) Makihara, N.; Ogo, S.; Watanabe, Y. *Organometallics* **2001**, *20*, 497−500. (c) Ogo, S.; Makihara, N.; Watanabe, Y. *Organometallics* **1999**, *18*, 5470−5474.

(3) (a) Haack, K.-J.; Hashiguchi, S.; Fujii, A.; Ikariya, T.; Noyori, R. *Angew. Chem., Int. Ed. Engl.* **1997**, *36*, 285−288. (b) Fujii, A.; Hashiguchi, S.; Uematsu, N.; Ikariya, T.; Noyori, R. *J. Am. Chem. Soc.* **1996**, *118*, 2521−2522. (c) Uematsu, N.; Fujii, A.; Hashiguchi, S.; Ikariya, T.; Noyori, R. *J. Am. Chem. Soc.* **1996**, *118*, 4916−4917. (d) Menashe, N.; Shov, Y. *Organometallics* **1991**, *10*, 3885−3891. (e) Menashe, N.; Salant, E.; Shov, Y. *J. Organomet. Chem.* **1996**, *514*, 97−102. (f) Casey, C. P.; Singer, S. W.; Powell, D. R.; Hayashi, R. K.; Kavana, M. *J. Am. Chem. Soc.* **2001**, *123*, 1090−1100. (g) Katho, A.; Carmona, D.; Viguri, F.; Remacha, C. D.; Kovacs, J.; Joo, F.; Oro, L. A. *J. Organomet. Chem.* **2000**, *593/594*, 299−306. (h) Watanabe, Y.; Ohta, T.; Tsuji, Y. *Bull. Chem. Soc. Jpn.* **1982**, *55*, 2441−2444. (i) Rhyoo, H. Y.; Park, H.-J.; Chung. Y. K. *Chem. Commun.* **2001**, 2064−2065. (j) Lo, H. C.; Buriez, O.; Kerr, J. B.; Fish, R. H. *Angew. Chem., Int. Ed.* **1999**, *38*, 1429−1432.

(4) Dadci, L.; Elias, H.; Frey, U.; Hornig, A.; Koelle, U.; Merbach A. E.; Paulus H.; Schneider J. S. *Inorg. Chem.* **1995**, *34*, 306−315.

(5) Casey, C. P.; Singer, S. W.; Powell, D. R. *Can. J. Chem.* **2001**, *79*, 1002−1011.

(6) (a) Jahncke, M.; Meister, M.; Rheinwald, G.; Stoeckli-Evans, J.; Suss-Fink, G. *Organometallics* **1997**, *16*, 1137−1143. (b) Stebler-Rothlisberger, M.; Ludi, A. *Polyhedron* **1986**, *5*, 1217−1221.

10.1021/om011059x CCC: $22.00
Publication on Web 06/05/2002

Scheme 1

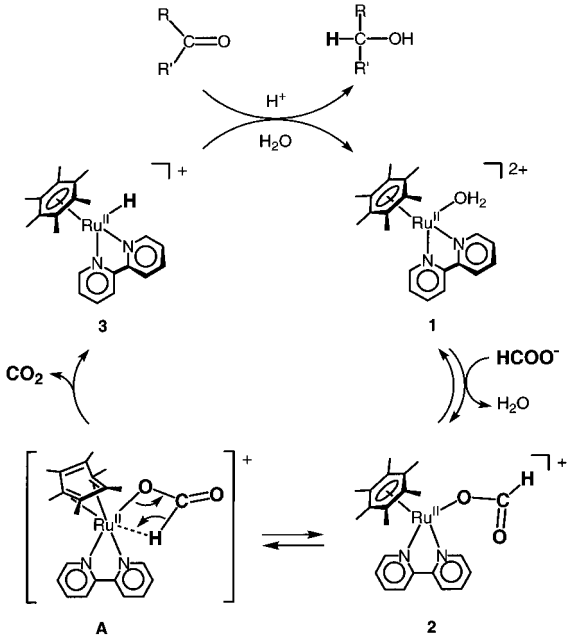

by coordination of one η^6-C_6Me_6 and three H_2O ligands. The average value of Ru−O bond lengths, 2.122 Å, in **4** is the same as that observed in $[Ru^{II}(H_2O)_6](C_7H_7SO_3)_2$.[8] It has been confirmed that complex **4** does not catalyze the transfer hydrogenation of the ketones examined in this study.

Catalyst Precursor $[(\eta^6\text{-}C_6Me_6)Ru^{II}(bpy)(H_2O)]^{2+}$ (1). The catalyst precursor **1**(SO_4) was quantitatively synthesized from the reaction of **4**(SO_4) with bpy at pH 3.8 in water. The structure of **1**$(PF_6)_2$ was determined by X-ray analysis (Figure 2).[9] Complex **1** adopts a distorted-octahedral coordination which is surrounded by one η^6-C_6Me_6, one bpy, and one H_2O ligand. The Ru−O bond length is 2.153(2) Å. The torsion angle between the least-squares plane of η^6-C_6Me_6 and that of bpy is 52.5(1)°. Koelle et al. have reported that the pK_a value of the aqua ligand of **1** is 7.3 (eq 1).[4] The aqua

$$[(\eta^6\text{-}C_6Me_6)Ru^{II}(bpy)(H_2O)]^{2+} \overset{pK_a = 7.3}{\rightleftharpoons} [(\eta^6\text{-}C_6Me_6)Ru^{II}(bpy)(OH)]^{+} + H^{+} \quad (1)$$

complexes **1** and **4** have high solubility in water (**1**, 136.2 mg/mL at pH 3.0; **4**, 113.8 mg/mL at pH 2.5 at 25 °C). It is noteworthy that complexes **1** and **4** are thermally stable and no decomposition is observed in water at temperatures up to 100 °C.

Intermediate $[(\eta^6\text{-}C_6Me_6)Ru^{II}(bpy)(HCOO)]^{+}$ (2) and the Catalyst $[(\eta^6\text{-}C_6Me_6)Ru^{II}(bpy)H]^{+}$ (3). In the absence of the reducible ketones, as a function of pH, complex **1** reacts with HCOONa to provide the formato

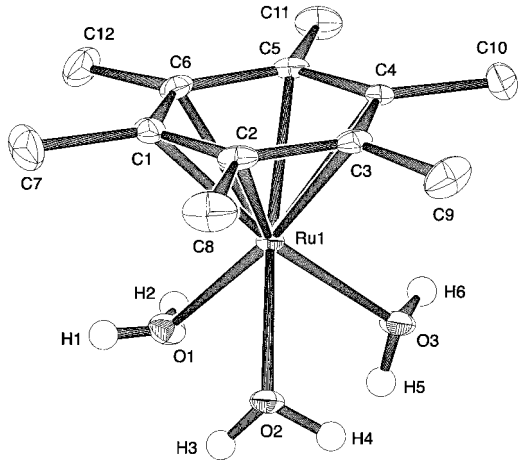

Figure 1. ORTEP drawing of **4**. The anion (SO_4) and hydrogen atoms of η^6-C_6Me_6 are omitted for clarity. Selected bond lengths (l/Å) and angles (ϕ/deg): Ru1−O1 = 2.126(2), Ru1−O2 = 2.150(2), Ru1−O3 = 2.091(2), Ru1−C1 = 2.192(2), Ru1−C2 = 2.181(2), Ru1−C3 = 2.159(2), Ru1−C4 = 2.174(2), Ru1−C5 = 2.174(2), Ru1−C6 = 2.160(2), O1−Ru1−O2 = 82.90(7), O1−Ru1−O3 = 81.25(8), O2−Ru1−O3 = 81.25(7).

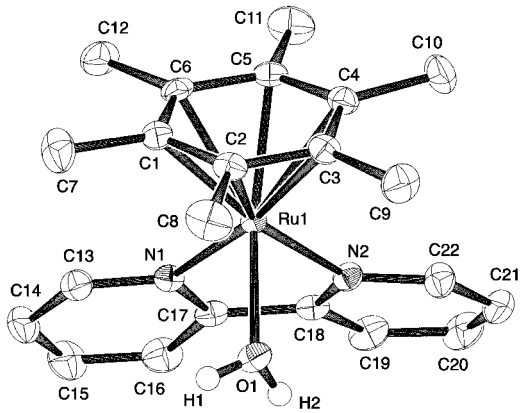

Figure 2. ORTEP drawing of **1**. The anions (PF_6) and hydrogen atoms of η^6-C_6Me_6 and bpy are omitted for clarity. Selected bond lengths (l/Å) and angles (ϕ/deg): Ru1−O1 = 2.153(2), Ru1−N1 = 2.096(2), Ru1−N2 = 2.099(3), Ru1−C1 = 2.228(3), Ru1−C2 = 2.205(3), Ru1−C3 = 2.235(3), Ru1−C4 = 2.239(3), Ru1−C5 = 2.181(3), Ru1−C6 = 2.202(3), O1−Ru1−N1 = 85.29(10), O1−Ru1−N2 = 84.52(10), N1−Ru1−N2 = 76.67(10)

complex **2** as the intermediate of β-hydrogen elimination and the hydrido complex **3** as the catalyst for the transfer hydrogenation (see Experimental Section). The structure of **2**(HCOO)·HCOOH was determined by X-ray analysis (Figure 3).[10] Complex **2** adopts a distorted-octahedral structure; it is surrounded by one η^6-C_6Me_6, one bpy, and one monodentate $HCOO^-$ ligand. Recently, Casey et al. have reported a crystal structure of a formato complex as an intermediate of β-hydrogen elimination of the formato ion.[5] Figure 4a shows the ^1H NMR spectrum (in D_2O at 25 °C at pD 4.5)[11] of the reaction mixture of **1**, **2**, and **3** that is in situ prepared

(7) Crystal data for **4**(SO_4)·$3H_2O$: $C_{12}H_{30}O_{10}RuS$, MW 467.49, triclinic, space group $P\bar{1}$ (No. 2), a = 8.5820(0) Å, b = 10.4284(4) Å, c = 11.0395(2) Å, α = 86.80(1)°, β = 67.95(1)°, γ = 74.53(1)°, V = 881.43(9) Å^3, Z = 2, D_c = 1.761 g cm^{-3}, μ(Mo Kα) = 10.56 cm^{-1}, R = 0.026, and R_w = 0.061.

(8) Rernhard, P.; Burge, H.-B.; Hauser, J.; Lehmann, H.; Ludi. A. *Inorg. Chem.* **1982**, *21*, 3936−3941.

(9) Crystal data for **1**$(PF_6)_2$: $C_{22}H_{28}F_{12}N_2OP_2Ru$, MW 727.47, monoclinic, space group $P2_1/n$ (No. 14), a = 10.4363(8) Å, b = 14.969(1) Å, c = 16.966(1) Å, β = 92.079(4)°, V = 2648.7(3) Å^3, Z = 4, D_c = 1.824 g cm^{-3}, μ(Mo Kα) = 8.19 cm^{-1}, R = 0.037, and R_w = 0.092.

(10) Crystal data for **2**(HCOO)·HCOOH: $C_{25}H_{30}N_2O_6Ru$, MW 555.59, monoclinic, space group $P2_1/n$ (No. 14), a = 9.1194(5) Å, b = 14.5247(8) Å, c = 17.880(1) Å, β = 94.482(3)°, V = 2361.1(2) Å^3, Z = 4, D_c = 1.563 g cm^{-3}, μ(Mo Kα) = 7.08 cm^{-1}, R = 0.028, and R_w = 0.064.

(11) pD = pH meter reading +0.4. (a) Glasoe, P. K.; Long, F. A. *J. Phys. Chem.* **1960**, *64*, 188−190. (b) Mikkelsen, K.; Nielsen, S. O. *J. Phys. Chem.* **1960**, *64*, 632−637.

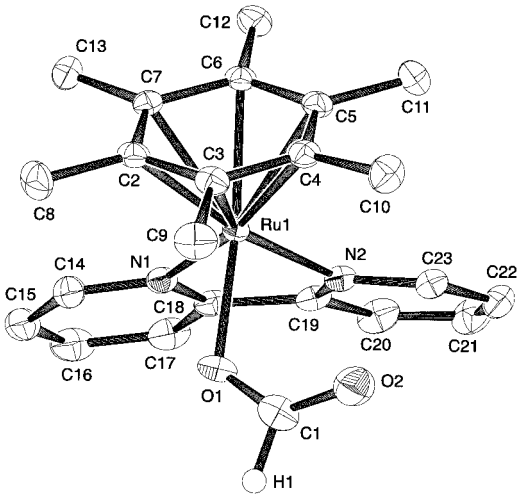

Figure 3. ORTEP drawing of **2**. The anion (HCOO) and hydrogen atoms of η^6-C_6Me_6 and bpy are omitted for clarity. Selected bond lengths (l/Å) and angles (ϕ/deg): Ru1−O1 = 2.107(2), Ru1−N1 = 2.084(2), Ru1−N2 = 2.094(2), O1−C1 = 1.250(3), O2−C1 = 1.229(3), C1−H1 = 1.05(3), Ru1−C2 = 2.218(2), Ru1−C3 = 2.199(2), Ru1−C4 = 2.251(2), Ru1−C5 = 2.204(2), Ru1−C6 = 2.209(2), Ru1−C7 = 2.218-(2), O1−Ru1−N1 = 80.38(7), O1−Ru1−N2 = 87.14(7), N1−Ru1−N2 = 76.45(7), Ru1−O1−C1 = 122.6(2), O1−C1−O2 = 129.5(2), O1−C1−H1 = 107(1), O2−C1−H1 = 122(1).

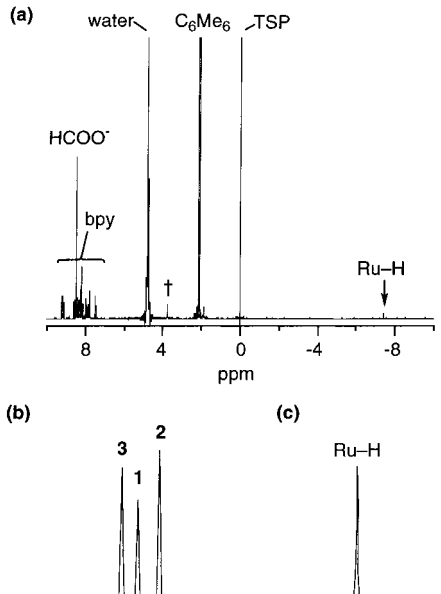

Figure 4. (a) ^{1}H NMR spectrum of the reaction mixture of **1**, **2**, and **3** in D_2O at 25 °C at pD 4.5. TSP: the reference with the methyl proton resonance set at 0.00 ppm. †: an impurity. ^{1}H NMR (270 MHz, in D_2O, reference to TSP): **2**: δ 2.09 (s, 18H), 7.78 (t, 2H), 8.17 (t, 2H), 8.29 (d, 2H), 9.20 (d, 2H) and **3**: δ 2.14 (s, 18H), 7.48 (t, 2H), 7.93 (t, 2H), 8.19 (d, 2H), 8.57 (d, 2H), −7.45 (s). (b) The signals derived from the C_6Me_6 ligands of **1**, **2**, and **3**. (c) The signal derived from the hydrido ligand of **3**.

from the reaction of **1** with HCOONa in D_2O.[2a,12] The signals around 2.1 ppm (Figure 4b) correspond to the

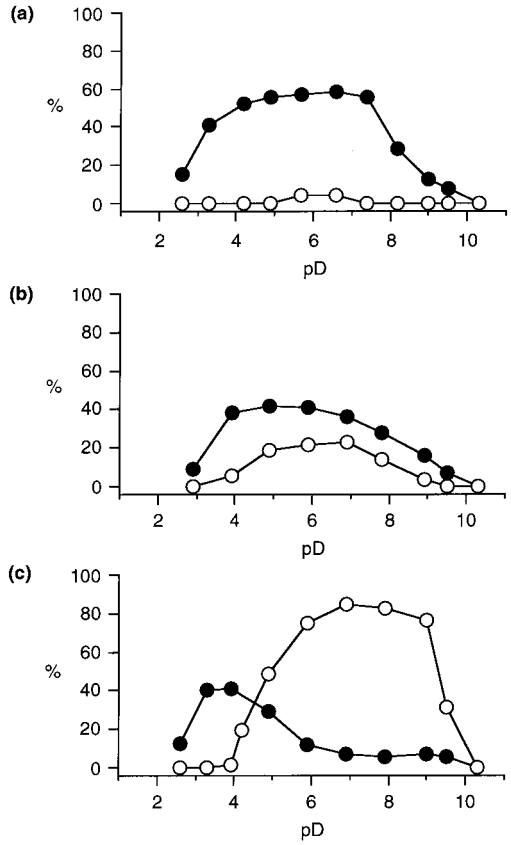

Figure 5. pD-dependent formation ratio of **2** (●) and **3** (○) in the reaction mixtures prepared by the reactions of **1**(SO_4) (5 μmol) with 10 equiv (50 μmol) of HCOONa in D_2O (1 mL) at 25 °C (a), 45 °C (b), and 70 °C (c) for 5 min.

protons of η^6-C_6Me_6 of **1** (2.13 ppm), **2** (2.09 ppm), and **3** (2.14 ppm). The signal at −7.45 ppm (Figure 4c) corresponds to the hydrido ligand of **3**.

Figure 5a−c shows the pD-dependent formation ratio of **2** (●) and **3** (○) from the reaction of **1**(SO_4) (5 μmol) with 10 equiv (50 μmol) of HCOONa (in the absence of the reducible ketones) in D_2O (1 mL) at 25 °C (Figure 5a), 45 °C (Figure 5b), and 70 °C (Figure 5c) for 5 min. As shown in Figure 5a, at 25 °C, complex **2** is formed in a pH range of about 3−9. This pH-dependence is rationalized as follows: (i) the pK_a value of HCOOH at the studied concentration is 3.6; thus, above pH 3.6, HCOONa acts as $HCOO^-$ to bind the ruthenium center, and (ii) the pK_a value of **1** is 7.3; thus, above pH 7.3, complex **1** is predominantly deprotonated to form a hydroxo complex $[(\eta^6\text{-}C_6Me_6)Ru^{II}(bpy)(OH)]^+$, which does not react with HCOONa. Figure 5b,c shows that the formation of **3** increases with an increase in temperature in a range of pH about 5−9, and the increase of the formation of **3** correlates with the decrease in the formation of **2**. Above 40 °C and below pD 6.0, the evolution of CO_2 and H_2 is confirmed by GC analysis. The evolution of H_2 most likely occurs from the reaction of the hydrido ligand (H^-) of **3** with H^+ in water (i.e., hydride protonation).

Figure S1a−c (in Supporting Information) shows the pD-dependent formation ratio of **2** (●) and **3** (○) from the reaction of **1**(SO_4) (5 μmol) with 10 equiv (50 μmol, Figure S1a), 100 equiv (500 μmol, Figure S1b), and 250 equiv (1.25 mmol, Figure S1c) of HCOONa (in the absence of the reducible ketones) in D_2O (1 mL) at 70

(12) Steckhan, E.; Herrman, S.; Ruppert, R.; Dietz, E.; Frede, M.; Spika, E. *Organometallics* **1991**, *10*, 1568−1577.

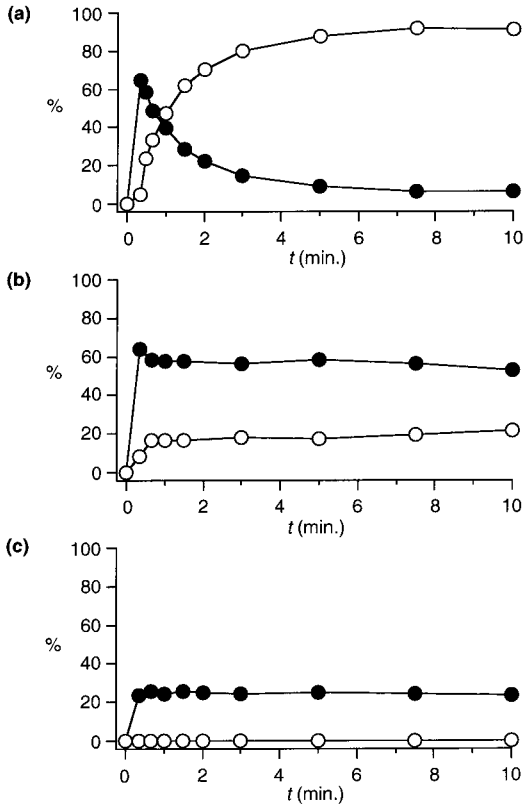

Figure 6. Time course of the formation ratio of **2** (●) and **3** (○) in the reaction mixtures prepared by the reactions of **1**(SO_4) (5 μmol) with 100 equiv (500 μmol) of HCOONa in D_2O (1 mL) at 70 °C at pD 7.5 (a), pD 4.3 (b), and pD 2.4 (c).

°C for 5 min. Figure 6a−c shows the time course of the formation ratio of **2** (●) and **3** (○) from the reaction of **1**(SO_4) (5 μmol) with 100 equiv (500 μmol) of HCOONa (in the absence of the reducible ketones) in D_2O (1 mL) at 70 °C at pD 7.5 (Figure 6a), pD 4.3 (Figure 6b), and pD 2.4 (Figure 6c). As shown in Figure 6a, above pD 6.0, the time-dependent formation of **3** that correlates with the decrease in the formation of **2** is observed without evolution of H_2 gas.

pH-Dependent Transfer Hydrogenation in Water. We here demonstrate pH-dependent transfer hydrogenation of water-soluble ketones with **1**(SO_4) and HCOONa in water at 25−90 °C. The series of water-soluble ketones includes examples of a cyclic ketone (cyclohexanone: **a**), a straight chain ketone (2-butanone: **b**), a keto-acid (pyruvic acid: **c**), and an acetophenone (as a water-insoluble ketone) derivative with a water-soluble ligand (4-acetylbenzenesulfonic acid sodium salt: **d**) (Table 1). Products were determined by ^{1}H NMR. Turnover frequency (TOF) is expressed as the number of moles of product formed per mole of catalyst per 1 h. The average TOFs were determined by ^{1}H NMR analysis of the reaction mixture samples (based on the ketones and the products). It has been confirmed that the transfer hydrogenation does not occur in the absence of **1** or HCOONa.

As shown in Table 1 (conditions of the transfer hydrogenation: pH 4.0, 6000 equiv of HCOONa, 70 °C), the cyclic ketone (**a**) is converted to the corresponding alcohol much more efficiently than the straight chain ketone (**b**). The transfer hydrogenation of the keto-acid

Table 1. Transfer Hydrogenation of Water-Soluble Carbonyl Compounds (a−d) and Water-Insoluble Carbonyl Compounds (e−g) with $[(\eta^6\text{-}C_6Me_6)Ru^{II}(bpy)(H_2O)]^{2+}$ as a Catalyst Precursor and HCOONa as a Hydrogen Donor in Water and in Biphasic Media at pH 4.0[a]

	substrate	product	TOF[b,c]	t(h)	yield(%)[c]
(a)			98	4	99
(b)	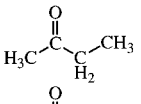	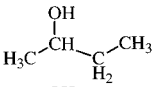	58	6	97
(c)	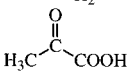	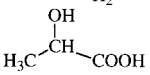	96	4	99
(d)	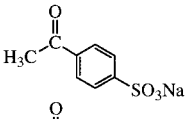	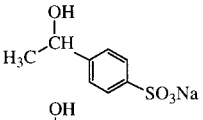	103	3	98
(e)	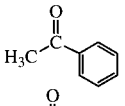	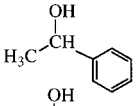	75	4	98
(f)	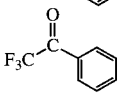	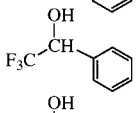	153	4	99
(g)			21	13	97

[a] The reaction was carried out at 70 °C using a ketone (0.32 mmol) in H_2O (3 mL) with **1**/ketone/HCOONa = 1/200/6000. [b] Turnover frequency: (mol of product/mol of **1**)/h. [c] Detected by ^{1}H NMR analysis.

(**c**) also occurs easily. The rate of the transfer hydrogenation of the water-soluble acetophenone derivative (**d**) in water is faster than that of acetophenone (**e**) in biphasic media. Interestingly, the rate of the transfer hydrogenation of **a**−**d** in water shows a sharp maximum around pH 4.0. In Figure 7a, ▼ shows pH-dependent profiles of the transfer hydrogenation of **a** (100 μmol) with **1**(SO_4) (5 μmol) and 100 equiv (500 μmol) of HCOONa in water (1 mL) at 70 °C for 5 min and ■ shows that of **a** (0.32 mmol) with **1**(SO_4) (1.6 μmol) and 6000 equiv (9.6 mmol) of HCOONa in water (3 mL) at 70 °C for 1 h. In Figure 8a, ■ shows TOFs depending upon the number of moles of HCOONa in the transfer hydrogenation of **a**. In Figure 8b, ■ shows temperature-dependent TOFs in the transfer hydrogenation of **a**. In Figure 8c, ■ shows the time course of the TONs in the transfer hydrogenation of **a**.

pH-Dependent Transfer Hydrogenation in Biphasic Media. We also demonstrate pH-dependent transfer hydrogenation of water-insoluble ketones with **1**(SO_4) and HCOONa in biphasic media at 25−90 °C. The examples of water-insoluble ketones examined in this study are acetophenone (**e**), an acetophenone derivative containing an electron-withdrawing group (2,2,2-trifluoroacetophenone: **f**), and a bulky ketone (alpha-tetralone: **g**) (Table 1). The rate of the transfer hydrogenation of **e**−**g** in biphasic media also shows a sharp maximum around pH 4.0 (in the case of biphasic media, the pH value of the aqueous phase is adopted). In Figure 7b, ▽ shows pH-dependent profiles of the transfer hydrogenation of **e** (100 μmol) with **1**(SO_4) (5 μmol) and 100 equiv (500 μmol) of HCOONa in water

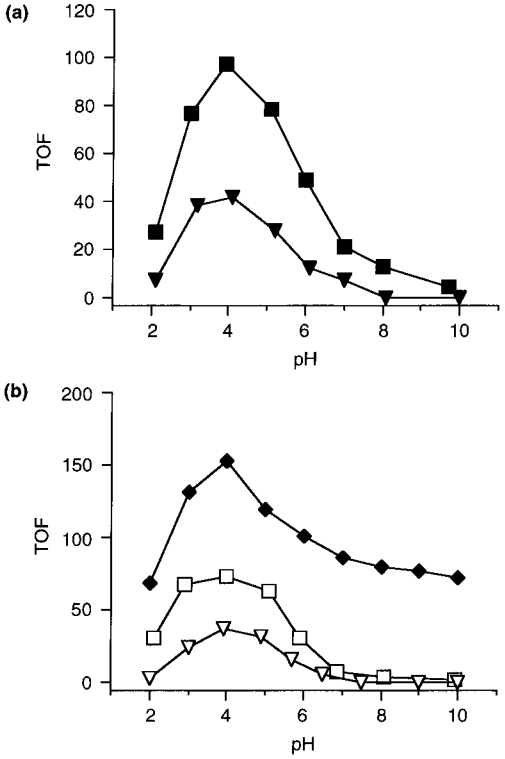

Figure 7. (a) ▼: pH-dependent profiles of the transfer hydrogenation of **a** (100 μmol) with **1**(SO_4) (5 μmol) and 100 equiv (500 μmol) of HCOONa in water (1 mL) at 70 °C for 5 min. ■: pH-dependent profiles of the transfer hydrogenation of **a** (0.32 mmol) with **1**(SO_4) (1.6 μmol) and 6000 equiv (9.6 mmol) of HCOONa in water (3 mL) at 70 °C for 1 h. (b) ▽: pH-dependent profiles of the transfer hydrogenation of **e** (100 μmol) with **1**(SO_4) (5 μmol) and 100 equiv (500 μmol) of HCOONa in water (1 mL) at 70 °C for 5 min. □: pH-dependent profiles of the transfer hydrogenation of **e** (0.32 mmol) with **1**(SO_4) (1.6 μmol) and 6000 equiv (9.6 mmol) of HCOONa in water (3 mL) at 70 °C for 1 h. ◆: pH-dependent profiles of the transfer hydrogenation of **f** (0.32 mmol) with **1**(SO_4) (1.6 μmol) and 6000 equiv (9.6 mmol) of HCOONa in water (3 mL) at 70 °C for 1 h.

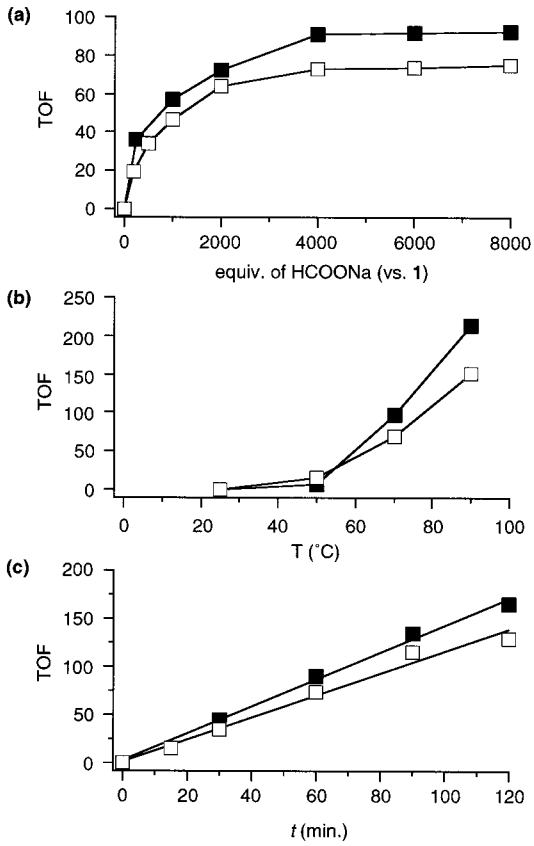

Figure 8. (a) ■: TOFs depending upon the number of moles of HCOONa of the transfer hydrogenation of **a.** □: TOFs depending upon the number of moles of HCOONa of the transfer hydrogenation of **e**. Conditions: **1**(SO_4) (1.6 μmol), 0−8000 equiv of HCOONa (0−12.8 mmol), 200 equiv of the substrate (0.32 μmol), and H_2O (3 mL). (b) ■: temperature-dependent TOFs of the transfer hydrogenation of **a**. □: temperature-dependent TOFs of the transfer hydrogenation of **e**. (c) ■: time course of the TONs of the transfer hydrogenation of **a**. □: time course of the TONs of the transfer hydrogenation of **e**.

(1 mL) at 70 °C for 5 min and □ shows that of **e** (0.32 mmol) with **1**(SO_4) (1.6 μmol) and 6000 equiv (9.6 mmol) of HCOONa in water (3 mL) at 70 °C for 1 h. In Figure 8a, □ shows TOFs depending upon the number of moles of HCOONa of the transfer hydrogenation of **e**. In Figure 8b, □ shows temperature-dependent TOFs of the transfer hydrogenation of **e**. In Figure 8c, □ shows the time course of the TONs of the transfer hydrogenation of **e**.

Mechanism for the pH-Dependent Transfer Hydrogenation. We propose a mechanism for the pH-dependent transfer hydrogenation as follows: above pH 3.6 (= the pK_a value of HCOOH), the aqua complex **1** reacts with $HCOO^-$ to provide the formato complex **2**. The hydrido complex **3** is generated through β-hydrogen elimination via a η^6- to η^4-arene coordination shift (a ring-slippage mechanism, **A**)[13] with the evolution of CO_2.[14] Then, complex **3** reacts with the ketones to give the corresponding alcohols. It was confirmed that at pH 4.0 at 70 °C the isolated **3** acts as the catalyst for the reduction of the ketones in the absence of HCOONa as the hydrogen donor (i.e., under stoichiometric conditions) and in the presence of excess amounts of HCOONa (i.e., under catalytic conditions). It is important to note that the isolated **2** does not act as the catalyst for the transfer hydrogenation of the ketones.

In the absence of the reducible ketones, the reaction of **1** with 100 equiv of HCOONa at 70 °C provides the catalyst **3** in the range of pH about 4−10 (Figure S1b). However, under the same conditions (100 equiv of HCOONa at 70 °C), in the presence of the reducible ketones, the rate of the transfer hydrogenation shows a maximum around pH 4.0 (e.g., ▼ and ▽ in Figure 7), namely, the pH-dependence of the transfer hydrogenation does not agree with the pH-profile of the formation of the catalyst **3**. This discrepancy reveals that the pH-dependence of the transfer hydrogenation is controlled not only by the stability of the catalyst in these acidic media but rather by the activation process of the ketones by protons (Figure 9).[3a−f,5] The activation process of the ketones should be dependent on the Lewis acidity of the carbonyl carbon that accepts a hydride ion from the catalyst. Therefore, as shown in Figure 7b, the transfer hydrogenation of **f** (the acetophenone derivative containing the electron-withdrawing group

(13) (a) O'Connor, J. M.; Casey, C. P. *Chem. Rev.* **1987**, *87*, 307−318. (b) Basolo, F. *New J. Chem.* **1994**, *18*, 19−24.

(14) The evolution of CO_2 was determined by GC analysis.

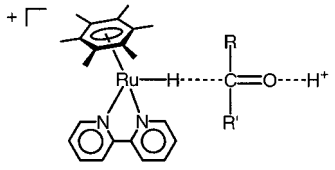

3

Figure 9. Mechanism for the hydrogen transfer.

of the carbonyl carbon, ◆) proceeds more efficiency than that of **e** (acetophenone, □) in the range of pH about 2−10.

Conclusions

We have demonstrated the potential of the organometallic aqua complex **1** to be a catalyst precursor for the pH-dependent transfer hydrogenation of water-soluble and -insoluble ketones in water and in biphasic media. In the absence of the reducible ketones, as a function of pH, the catalyst precursor **1** reacts with HCOONa to provide **2** as the intermediate of β-hydrogen elimination and **3** as the catalyst for the transfer hydrogenation. It was elucidated that the isolated **3** acts as the catalyst for the reduction of the ketones in H_2O at pH 4.0 at 70 °C, though the isolated **2** does not catalyze the transfer hydrogenation of the ketones in $CHCl_3$ at 60 °C. Interestingly, despite the solubility of the ketones toward water, the rate of the transfer hydrogenation shows a sharp maximum around pH 4.0. We have discussed this pH-dependence on the basis of the stability of the catalyst and the activation process of the ketones in the aqueous media.

Experimental Section

Materials and Methods. All reactions were carried out under Ar atmosphere, using standard Schlenk techniques and a glovebox. Deuterated solvents were purchased from Cambridge Isotope Laboratories, Inc. Chemicals (highest purity available) were purchased from Aldrich Chemicals Co. and used without further purification. Purification of water was performed with a Milli-Q system (Millipore; Milli-RO 5 plus and -Q plus). The ^{1}H NMR spectra were recorded on a JEOL JNM-EX 270 spectrometer at 20 °C. H_2 and CO_2 gases were determined by a Shimadzu GC-8A (He carrier, Unibeads column, 60/80 2 m, GL Sciences Inc.) equipped with a thermal conductivity detector.

pH-Adjustment. In a pH range of 1.0−13.0, the pH value of the solutions was determined by a pH meter (TOA, HM-18E) equipped with a pH combination electrode (TOA, GS-5015C). The pH of the solution was adjusted by using 0.01−3 M HNO_3/H_2O and 0.01−3 M $NaOH/H_2O$ without buffer. To determine the exact pH value, the ^{1}H NMR experiments were performed by using an NMR tube (diameter = 5.0 mm) with a sealed capillary tube (diameter = 1.5 mm) containing 3-(trimethylsilyl)propionic acid-2,2,3,3-d_4 sodium salt (TPS, as the reference with the methyl proton resonance set at 0.00 ppm) dissolved in D_2O (for deuterium lock). During the reaction, a stainless steel micro pH probe (IQ Scientific Instruments, Inc.; PH15-SS) was dipped in the reaction mixture at 70 °C in the Schlenk tube under Ar atmosphere and the pH of the solution was monitored by a pH meter (IQ Scientific Instruments, Inc.; IQ200).

[(η^6-C_6Me_6)Ru^{II}(bpy)(H_2O)](SO_4) {1(SO_4)}. 2,2′-Bipyridine (187.2 mg, 1.2 mmol) was added to a solution of [(η^6-C_6Me_6)Ru(H_2O)$_3$](SO_4) {**4**(SO_4), 496.1 mg, 1.2 mmol} in H_2O (100 mL). The yellow suspension was stirred for 12 h at ambient temperature, giving a pale orange solution. The solvent was evaporated to yield yellow microcrystalline **1**(SO_4), which was dried in vacuo {yield 90% based on **4**(SO_4)}. ^{1}H NMR (270 MHz, in D_2O at pD 3.8, reference to TSP, 25 °C): δ 2.13 (s, 18H), 7.88 (t, 2H), 8.20 (t, 2H), 8.40 (d, 2H), 9.16 (d, 2H). Anal. Calcd for **1**(PF_6)$_2$: $C_{22}H_{28}F_{12}N_2OP_2Ru$: C, 36.32; H, 3.88; N, 3.85. Found: C, 36.30; H, 3.82; N, 3.80.

[(η^6-C_6Me_6)Ru^{II}(bpy)(HCOO)](HCOO) {2(HCOO)}. The pH of a solution of **1**(SO_4) (53.3 mg, 0.1 mmol) and HCOONa (2.72 g, 40 mmol) in H_2O (20 mL) was adjusted to 4.0 by addition of 3 M HCOOH. The solution was stirred at 40 °C. After 30 min, the solution was extracted with $CHCl_3$ (5 × 10 mL). The orange organic phase was dried over Na_2SO_4. Upon evaporation of $CHCl_3$, an orange powder was obtained. The powder was recrystallized from $CHCl_3$/diethyl ether to provide air-sensitive orange needles of **2**(HCOO) {yield: 50% based on **1**(SO_4)}. ^{1}H NMR (270 MHz, in $CDCl_3$, reference to TMS, 25 °C): δ 2.10 (s, 18H), 7.67 (t, 2H), 7.79 (s, 1H), 8.16 (t, 2H), 8.46 (d, 2H), 9.14 (d, 2H).

[(η^6-C_6Me_6)Ru^{II}(bpy)H](PF_6) {3(PF_6)}. The pH of a solution of **1**(SO_4) (53.3 mg, 0.1 mmol) and HCOONa (680 mg, 10 mmol) in H_2O (15 mL) was adjusted to 8.0 by addition of 0.1 M NaOH. The solution was stirred at 70 °C. After 30 min, to the solution was added a solution of $NaPF_6$ (16.8 mg, 0.1 mmol) in H_2O (4 mL) at 70 °C to form a precipitate of **3**(PF_6), which was collected by filtration, washed with water, and dried in vacuo {yield 65% based on **1**(SO_4)}. Complex **3**(PF_6) is slightly dissolved in water. ^{1}H NMR (270 MHz, in D_2O, reference to TSP, 25 °C): δ 2.14 (s, 18H), 7.48 (t, 2H), 7.93 (t, 2H), 8.19 (d, 2H), 8.57 (d, 2H), −7.45 (s).

pH-Dependent Transfer Hydrogenation. pH-dependent transfer hydrogenation of water-soluble and -insoluble ketones (0.32 mmol) with **1**(SO_4) (1.6 μmol) and HCOONa (9.6 mmol) was carried out in H_2O (3 mL) at 25−90 °C under Ar atmosphere. The reaction was quenched by dropping the temperature of the mixture to 0 °C. In the case of biphasic media, the products were extracted by CH_2Cl_2. The products were determined by ^{1}H NMR.

X-ray Crystallographic Analysis. Crystallographic data for **1**(PF_6)$_2$, **2**(HCOO)·HCOOH, and **4**(SO_4)·3H_2O have been deposited with the Cambridge Crystallographic Data Center as supplementary publication no. CCDC-175507, -175508, -175509, respectively. Copies of the data can be obtained free of charge on application to CCDC, 12 Union Road, Cambridge CB21EZ, UK {fax: (+44)1223-336-033; e-mail: deposit@ccdc.cam.ac.uk}. Orange crystals of **1**(PF_6)$_2$ and **4**(SO_4)·3H_2O used in X-ray structure analysis were obtained from aqueous solutions of **1**(PF_6)$_2$ and **4**(SO_4) at pH 5.0 and 3.0, respectively. Orange crystals of **2**(HCOO)·HCOOH were obtained by diffusion of diethyl ether into a $CHCl_3$ solution of **2**(HCOO) at ambient temperature. Measurements were made on a Rigaku/MSC Mercury CCD diffractometer with graphite-monochromated Mo Kα radiation (λ = 0.7107). All calculations were performed using the teXsan crystallographic software package of Molecular Structure Corporation. Crystal data, data collection parameters, structure solution and refinement, atomic coordinates, anisotropic displacement parameters, bond lengths, and bond angles are given in Supporting Information.

Acknowledgment. Financial support of this research by the Ministry of Education, Science, Sports, and Culture, Japan Society for the Promotion of Science, Grants-in-Aid for Scientific Research to S.O. (13640568) and Y.W. (11490036 and 11228208), is gratefully acknowledged. We thank Professors K. Isobe (Osaka City University) and S. Fukuzumi (Osaka University) for valuable discussions.

Supporting Information Available: Figure S1 and crystallographic information. This material is available free of charge via the Internet at http://pubs.acs.org.

OM011059X